

# Synthetic circuits integrating logic and memory in living cells

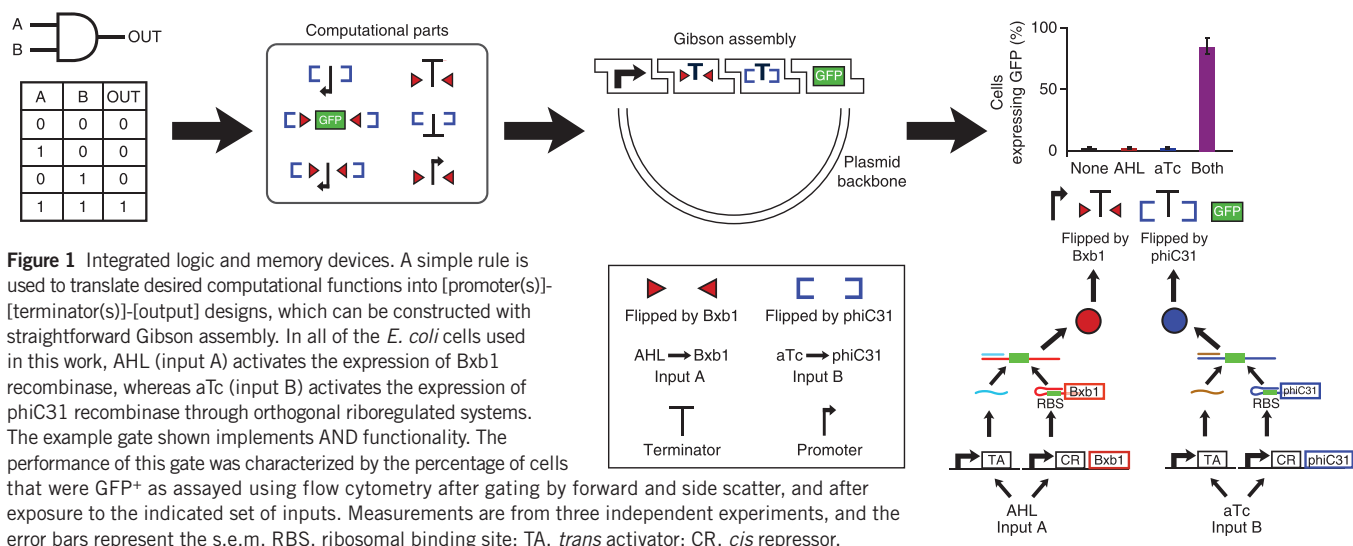
Piro Siuti<sup>1,2</sup>, John Yazbek<sup>3</sup> & Timothy K Lu<sup>1,2</sup>

Logic and memory are essential functions of circuits that generate complex, state-dependent responses. Here we describe a strategy for efficiently assembling synthetic genetic circuits that use recombinases to implement Boolean logic functions with stable DNA-encoded memory of events. Application of this strategy allowed us to create all 16 two-input Boolean logic functions in living *Escherichia coli* cells without requiring cascades comprising multiple logic gates. We demonstrate long-term maintenance of memory for at least 90 cell generations and the ability to interrogate the states of these synthetic devices with fluorescent reporters and PCR. Using this approach we created two-bit digital-to-analog converters, which should be useful in biotechnology applications for encoding multiple stable gene expression outputs using transient inputs of inducers. We envision that this integrated logic and memory system will enable the implementation of complex cellular state machines, behaviors and pathways for therapeutic, diagnostic and basic science applications.

A central goal of synthetic biology is to create cellular networks that integrate input signals for decision making and actuation<sup>1</sup>. In recent

years, artificial logic gates<sup>2–4</sup> and memory devices<sup>5–8</sup> have been independently constructed. In previous implementations of cellular logic, complex gates such as XOR and XNOR require the layering of multiple genetic circuits<sup>2,4</sup>, thus necessitating substantial efforts in circuit construction and tuning. Furthermore, these complex logic functions have not been connected to memory devices that can store the output of their computations and can thus only achieve combinatorial logic. However, integrated logic and memory are crucial for performing complex and persistent state-dependent computations such as sequential logic<sup>9</sup>. Here we present an efficient strategy for building synthetic logic circuits in single cells with concomitant DNA-encoded memory storage. DNA-based memory is a useful implementation of long-term storage, as it is naturally propagated when cells divide and can be stable even after cell death<sup>7,10</sup>.

To test this strategy, we used chemical-inducer inputs to drive the expression of orthogonal recombinases from inducible promoters. These recombinases target genetic components for DNA inversion, resulting in conditional gene expression. We then built all possible two-input logic functions by straightforward assembly of recombinase-targeted promoters, terminators and output gene modules in various orientations, enabling simple user-defined programming of cellular logic with memory (Fig. 1 and Supplementary Data).



<sup>1</sup>Department of Electrical Engineering and Computer Science, Massachusetts Institute of Technology, Cambridge, Massachusetts, USA. <sup>2</sup>Department of Biological Engineering, Massachusetts Institute of Technology, Cambridge, Massachusetts, USA. <sup>3</sup>Department of Chemical Engineering, Massachusetts Institute of Technology, Cambridge, Massachusetts, USA. Correspondence should be addressed to T.K.L. (timlu@mit.edu).

Received 25 October 2012; accepted 17 January 2013; published online 10 February 2013; doi:10.1038/nbt.2510

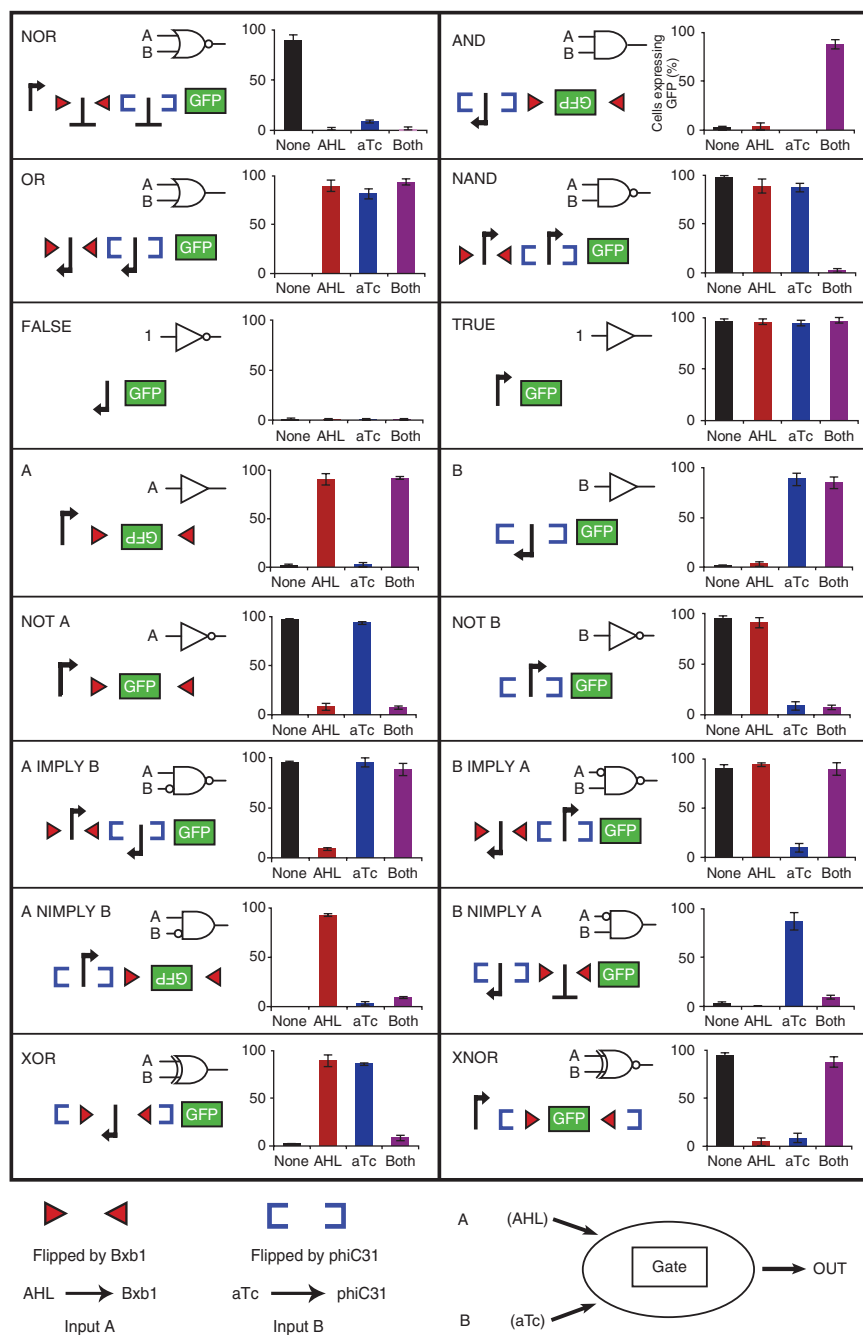
**Figure 2** Recombinase-based logic gates can implement a complete set of two-input-one-output Boolean logic gates without needing to cascade multiple universal gates together. Cells were exposed to no inputs, AHL only, aTc only, or AHL and aTc simultaneously. The performance of each logic gate was characterized by the percentage of cells that were GFP<sup>+</sup> as assayed using flow cytometry after gating by forward and side scatter. Measurements are from three independent experiments, and the error bars represent the s.e.m.

We used two serine recombinases, Bxb1 and phiC31, each of which targets its own cognate pair of nonidentical recognition sites known as *attB* and *attP*. Bxb1 and phiC31 can irreversibly invert or excise DNA on the basis of the orientation of the surrounding pair of recognition sites<sup>11</sup>. To ensure low leakage in the absence of inputs, we cloned *bxb1* (ref. 11) and *phiC31* (ref. 12) under the control of the inducible riboregulators *N*-Acyl homoserine lactone (AHL) and anhydrotetracycline (aTc)<sup>13</sup>, respectively. All cells contained both of these recombinase expression constructs and thus accept two digital inputs. When both AHL and aTc were used as inputs, they were applied simultaneously. Hereafter we refer to Bxb1 expression through AHL as signal A and phiC31 expression through aTc as signal B. We assayed the output of our logic and memory designs using *gfp* as a reporter gene (**Supplementary Fig. 1**). We verified that Bxb1 and phiC31 operate orthogonally with respect to each other (**Fig. 2**).

Recombinase-catalyzed inversion of cascaded promoters (recombinase-promoter logic) can implement OR or NAND logic, depending on the initial orientation of the promoters (**Fig. 2**). When both promoters are inverted with respect to the downstream output gene, flipping of either promoter by input A or B results in a high GFP output (OUT = A OR B). When both promoters are upright with respect to the downstream output gene, the inversion of both promoters by inputs A and B is required to produce a low output (OUT = A NAND B).

Recombinase-catalyzed inversion of cascaded unidirectional terminators (recombinase-terminator logic) can implement AND or NOR logic, depending on the initial orientation of the terminators (**Figs. 1 and 2**). When two terminators are upright and located between a promoter and an output gene, inversion of both terminators by inputs A and B results in a high output (OUT = A AND B). When two unidirectional terminators are initially inverted, the inversion of either terminator by input A or B results in a low output (OUT = A NOR B).

NOR and NAND gates are universal logic operations and can be assembled together to implement more complex functions<sup>14,15</sup>, as is often done in electrical systems. However, biological systems are resource-constrained environments with much fewer parts available for synthetic circuit design. Thus, direct and efficient



encoding of complex logic functions without the need to cascade multiple universal gates together is desirable.

By building different combinations of recombinase-invertible promoters, terminators and output genes, we created all 16 two-input Boolean logic functions in individual cells without requiring cascades comprising multiple logic gates (**Figs. 1 and 2**). We were able to do this using a modular one-step Gibson assembly strategy with reusable recombinase-invertible components<sup>16</sup>. A simple relationship defines the logic function implemented by a given design in the [promoter(s)]-[terminator(s)]-[output] structure (**Fig. 2**). Specifically, gene expression can occur only when at least one upstream promoter is upright AND no terminators are upright AND the output gene is upright. For example, B NIMPLY A is equivalent to B AND NOT A; this logic function can be built by cascading an inverted promoter, which is

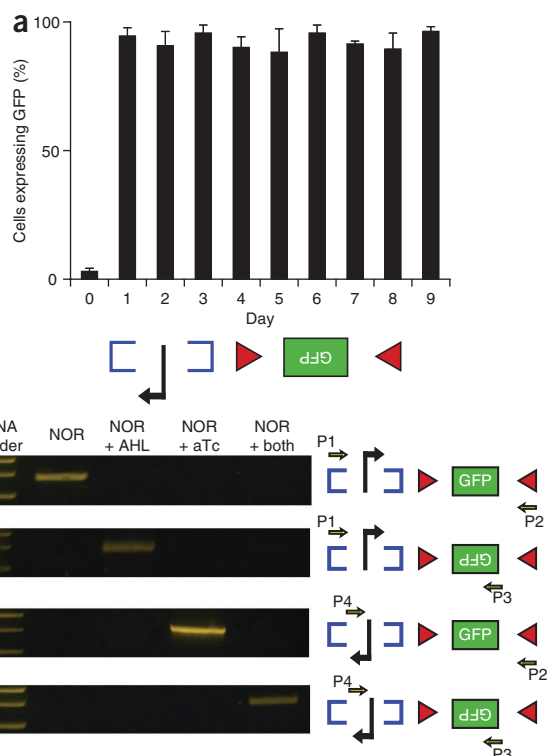
**Figure 3** Stable memory maintenance over multiple cell generations and after cell death. **(a)** Percentage of cells maintaining GFP expression, assayed by flow cytometry after gating by forward and side scatter, in cells containing an AND gate induced to the ON state after day 0 and continuously diluted and grown without input signals for 9 d thereafter. Measurements are from three independent experiments, and the error bars represent the s.e.m. **(b)** Each state of a NOR gate, as uniquely detected by PCR (yellow arrows indicate primers labeled as P1–P4) after cell death, and analysis of PCR products by electrophoresis on a 1% agarose gel.

flipped by phiC31 (after the addition of input B), with a downstream inverted unidirectional terminator, which is flipped by Bxb1 (after the addition of input A), and a downstream upright *gfp* output gene (Fig. 2). In this configuration, gene expression occurs only when B is TRUE (leading to an upstream promoter being upright) and A is FALSE (leading to no unidirectional terminators being upright).

Using these straightforward rules, a given logic function can be implemented using different combinations of the recombinase-invertible modules, thus giving flexibility for design (Figs. 1 and 2 and Supplementary Fig. 2). Complex XOR and XNOR gates can be implemented with the simplicity of the other logic gates by sandwiching components between the recombinase recognition sites of both recombinases (Fig. 2 and Supplementary Fig. 2). In the XOR gate in Figure 2, the double-sandwiched promoter is initially inverted. Any single inversion of the promoter (owing to either AHL or aTc) results in GFP expression, whereas no inversion of the promoter (owing to the absence of AHL and aTc) or double inversion of the promoter (owing to the presence of both AHL and aTc) results in the absence of GFP expression (Fig. 2). In the XOR gate in Supplementary Figure 2, a double-sandwiched *gfp* gene is initially inverted, and only single inversions of this gene owing to a single input result in GFP expression. In the XNOR gate, the double-sandwiched *gfp* gene is initially upright. Thus, the presence of a single input inverts the *gfp* gene and abolishes GFP expression, which would otherwise be present (Fig. 2).

As illustrated by the AND, XOR and NOR gates in Figures 1 and 2 and Supplementary Figure 2, multiple implementations of a given logic function can be built using our approach. Several factors may influence the choice of one implementation over the other alternatives: recombinase-catalyzed inversion efficiencies can vary based on DNA length<sup>17</sup>; leaky upstream and downstream gene-regulatory elements that are outside of the logic gate itself may affect the expression of output genes; the actual unidirectionality of the gene-regulatory elements may affect which components are used (for example, promoters may have transcriptional activity even in the inverted direction, or terminators may have transcriptional termination activity even in the inverted direction); and different recombinase recognition sites may affect the behavior of the gene-regulatory elements themselves.

A key feature of this computational paradigm is that these logic units maintain stable output memory after the inputs are withdrawn. We demonstrated this by allowing an AND gate to be induced to its ON state with both inputs and then repeatedly subdiluting and growing these cells for 9 d (>90 generations) without the inputs present (Fig. 3a). This circuit maintained a high output throughout the entire period after induction. This property should enable the creation of complex, state-dependent synthetic circuits. Furthermore, in contrast to circuits that use transcriptional or post-transcriptional logic, in our circuits we were able to detect the state of computations using PCR even after cell death (Fig. 3b). This feature may be used to create cellular biosensors whose states can be interrogated in a multiplexed fashion using high-throughput sequencing techniques.



One of the main goals of synthetic biology is to use synthetic gene circuits to develop higher-order networks with programmable functionality<sup>18</sup>. To demonstrate that our approach can be used to achieve this goal, we built digital-to-analog converters, which translate digital inducer inputs into stable analog gene expression outputs<sup>19</sup>. Our digital-to-analog converter circuits accept two digital inducer inputs (AHL and aTc) and produce four stable analog gene expression output levels on the basis of recombinase-invertible toggling of gene expression from constitutive promoters with different strengths (Fig. 4). We used three constitutive promoters (proA, proC and proD<sup>20</sup>) to build three distinct digital-to-analog converters with different digitally settable gene expression output levels. We determined the relative strengths of the variant promoters with downstream Bxb1 and phiC31 recombinase-recognition sites by assaying GFP fluorescence using flow cytometry (Supplementary Fig. 3). These results showed that the phiC31 *attB* site reduced GFP expression from all promoters compared with the Bxb1 *attB* site or with no intervening recombinase recognition site.

Each digital-to-analog circuit contains a pair of these variant constitutive promoters, each of which drives the expression of GFP only after inducible recombinase-mediated inversion. The total GFP output of the circuit when exposed to both inputs is approximately equal to the GFP output level when only AHL is present plus the GFP output level when only aTc is present (Fig. 4). When the individual analog output levels of each recombinase-invertible *gfp* expression cassette are designed to vary by twofold with each other, the digital-to-analog circuit output is determined by the inputs on the basis of a simple binary code. For example, the digital AHL input can be represented as the least-significant bit and the digital aTc input can be represented as the most-significant bit in a binary integer that is scaled to yield the ultimate analog gene expression output (Fig. 4c).

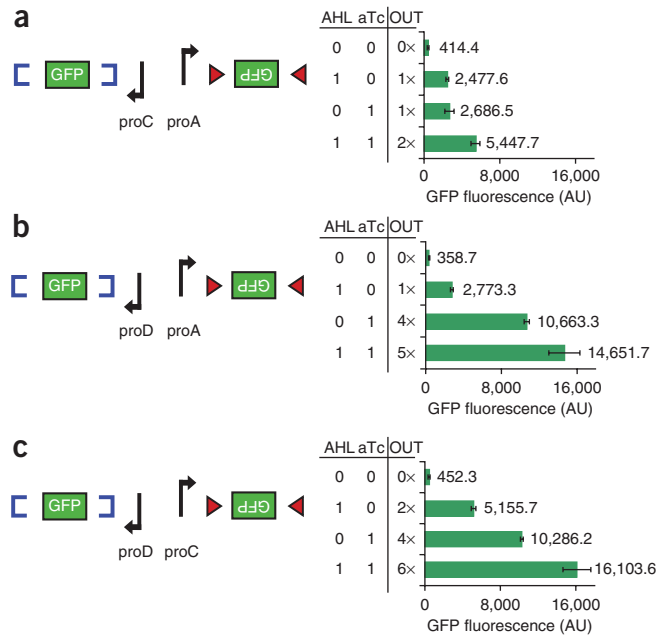
Beyond being a circuit motif for synthetic biology that to our knowledge has not been implemented before, we believe that the digital-to-analog circuit motif will be applicable to real-world applications.

**Figure 4** Recombinase-based logic and memory can implement digital-to-analog converters. Cells were exposed to no inputs, AHL only, aTc only, or AHL and aTc simultaneously. (a–c) Various digital combinations of the input inducers result in multiple levels of analog gene expression outputs on the basis of the varying strengths of the promoters used and the sum of their respective outputs. Non-normalized mean expression levels are given to the right of each bar in arbitrary units (AU) of fluorescence, and normalized expression levels are listed in the column labeled OUT, where they are rounded to the nearest integer, and 1× corresponds to ~2,700 AU. Fluorescence levels of the digital-to-analog converters with no inputs are very low on the basis of comparisons to control circuits that lack the *gfp* gene and cells that contain the *gfp* gene with an inverted promoter (**Supplementary Fig. 4**). Measurements of fluorescence values are based on geometric means from three independent experiments, and the error bars represent the s.e.m.

In particular, in biotechnology processes, constitutive promoters are useful for stable gene expression but suffer from the inability to dynamically tune gene expression levels or induce gene expression at defined time points<sup>21</sup>. In contrast, inducible promoters provide adjustable gene expression but rely on inducers that can be expensive or difficult to scale into higher volumes<sup>21</sup>. Our digital-to-analog converters provide an advantageous compromise between constitutive and inducible promoters and can be extended to enable the scalable programming of  $2^n$  constitutive output expression levels by the application of  $n$  input inducers. Cells containing these circuits need only be induced transiently to lock them into a defined constitutive level of expression, thus mitigating issues associated with inducer scalability. Digital-to-analog circuits may also be useful for multiplexed reporting of digital events with a single analog output. For example, distinct analog expression levels can be uniquely mapped back to their digital input combinations by a simple binary code (**Fig. 4c**).

We have created an efficient system for integrated logic and memory within single cells. Our modular DNA assembly strategy enables straightforward plug-and-play encoding of logic functions with concomitant memory arising from the ability of recombinases to ‘write’ information in DNA. This approach could be further applied to higher organisms, including eukaryotes. The complexity of single-cell logic and memory can be expanded by mining databases for new orthogonal recombinases or designing synthetic recombinases with defined DNA specificities<sup>22,23</sup>. Moreover, the simple rules that govern the behavior of recombinase-based computation should be compatible with automated genetic circuit design algorithms<sup>24</sup>. Complex multilayered circuits that perform state-dependent computation could be further designed by having the outputs of our circuits be recombinases or regulatory elements (for example, transcription factors or RNAs) that control downstream computational elements. Our recombinase-based circuits could target DNA carried on mobile genetic elements such as engineered bacteriophages as a form of portable and transmissible memory<sup>25,26</sup>. Future challenges associated with increasing the complexity of recombinase-based circuits will include explicitly validating orthogonality between recombinases as well as between recombinases and host genomes, engineering orthogonal recombinase expression vectors with minimal leakage<sup>13</sup>, accounting for timing issues in multilayer circuits or circuits that involve intercellular communication<sup>2,4,27,28</sup> and minimizing unwanted effects of recombinase recognition sites on the performance of regulatory components (for example, by using synthetic insulators).

Because we used unidirectional recombinases, our logic gates maintain memory of their inputs over time and are not conditional solely on their inputs at a given time. This useful property can enable the construction of biological-state machines that implement sequential logic and stable cellular states. For example, this platform could be used to build autonomous cellular circuits that transition cells in a



bioprocess through defined cellular phases, such as biomass accumulation followed by biomolecule production and then cell lysis. Cellular biosensors containing logic-and-memory circuits based on irreversible recombinases could be interrogated for their history of exposure to individual or logical combinations of environmental signals. For basic scientific applications, this framework could be used to establish stable synthetic differentiation cascades by controlling both the timing and sequence of transcription factors that determine cell fate. Dynamic cellular signals can be integrated into higher-order computations by linking them to recombinase expression. Multicellular systems endowed with these logic and memory devices may also implement distributed computation or synthetic cellular consortia<sup>27–29</sup>. By extending this approach to reversible memory devices<sup>7,8,19</sup>, one may be able to further construct sequential logic systems with resettable memory or clocked behaviors. However, a key challenge with reversible recombinase-memory devices is ensuring that transitions between states can be tightly controlled<sup>7,8,10</sup>. Ultimately, we envision that our approach for integrating cellular logic and memory will enable the construction of complex cellular state machines for biotechnology, therapeutic, diagnostic and basic science applications.

## METHODS

Methods and any associated references are available in the [online version of the paper](#).

*Note: Supplementary information is available in the online version of the paper.*

## ACKNOWLEDGMENTS

The *bxb1* gene was a generous gift from G.F. Hatfull (Department of Biological Sciences, University of Pittsburgh), and the riboregulator plasmids were donated by J.J. Collins (Biomedical Engineering, Boston University). The authors thank R. Daniai and A.A. Cheng for careful comments on the manuscript. This work was supported by an Office of Naval Research Multidisciplinary University Research Initiative (MURI) grant and the Defense Advanced Research Projects Agency (DARPA).

## AUTHOR CONTRIBUTIONS

T.K.L. conceived of this study. P.S. and J.Y. implemented, constructed and performed all experiments. All authors analyzed the data, discussed results and wrote the manuscript.

## COMPETING FINANCIAL INTERESTS

The authors declare competing financial interests: details are available in the [online version of the paper](#).

Published online at <http://www.nature.com/doi/10.1038/nbt.2510>.

Reprints and permissions information is available online at <http://www.nature.com/reprints/index.html>.

1. Hasty, J., McMillen, D. & Collins, J.J. Engineered gene circuits. *Nature* **420**, 224–230 (2002).
2. Regot, S. *et al.* Distributed biological computation with multicellular engineered networks. *Nature* **469**, 207–211 (2011).
3. Auslander, S., Auslander, D., Muller, M., Wieland, M. & Fussenegger, M. Programmable single-cell mammalian biocomputers. *Nature* **487**, 123–127 (2012).
4. Tamsir, A., Tabor, J.J. & Voigt, C.A. Robust multicellular computing using genetically encoded NOR gates and chemical 'wires'. *Nature* **469**, 212–215 (2011).
5. Ajo-Franklin, C.M. *et al.* Rational design of memory in eukaryotic cells. *Genes Dev.* **21**, 2271–2276 (2007).
6. Gardner, T.S., Cantor, C.R. & Collins, J.J. Construction of a genetic toggle switch in *Escherichia coli*. *Nature* **403**, 339–342 (2000).
7. Friedland, A.E. *et al.* Synthetic gene networks that count. *Science* **324**, 1199–1202 (2009).
8. Bonnet, J., Subsoontorn, P. & Endy, D. Rewritable digital data storage in live cells via engineered control of recombination directionality. *Proc. Natl. Acad. Sci. USA* **109**, 8884–8889 (2012).
9. Benenson, Y. Biomolecular computing systems: principles, progress and potential. *Nat. Rev. Genet.* **13**, 455–468 (2012).
10. Ham, T.S., Lee, S.K., Keasling, J.D. & Arkin, A.P. Design and construction of a double inversion recombination switch for heritable sequential genetic memory. *PLoS ONE* **3**, e2815 (2008).
11. Ghosh, P., Pannunzio, N.R. & Hatfull, G.F. Synapsis in phage Bxb1 integration: selection mechanism for the correct pair of recombination sites. *J. Mol. Biol.* **349**, 331–348 (2005).
12. Groth, A.C., Olivares, E.C., Thyagarajan, B. & Calos, M.P. A phage integrase directs efficient site-specific integration in human cells. *Proc. Natl. Acad. Sci. USA* **97**, 5995–6000 (2000).
13. Callura, J.M., Cantor, C.R. & Collins, J.J. Genetic switchboard for synthetic biology applications. *Proc. Natl. Acad. Sci. USA* **109**, 5850–5855 (2012).
14. Tabor, J.J. *et al.* A synthetic genetic edge detection program. *Cell* **137**, 1272–1281 (2009).
15. Rinaudo, K. *et al.* A universal RNAi-based logic evaluator that operates in mammalian cells. *Nat. Biotechnol.* **25**, 795–801 (2007).
16. Gibson, D.G. *et al.* Enzymatic assembly of DNA molecules up to several hundred kilobases. *Nat. Methods* **6**, 343–345 (2009).
17. Ringrose, L., Chabanis, S., Angrand, P.O., Woodroffe, C. & Stewart, A.F. Quantitative comparison of DNA looping *in vitro* and *in vivo*: chromatin increases effective DNA flexibility at short distances. *EMBO J.* **18**, 6630–6641 (1999).
18. Cheng, A.A. & Lu, T.K. Synthetic biology: an emerging engineering discipline. *Annu. Rev. Biomed. Eng.* **14**, 155–178 (2012).
19. Lu, T.K., Khalil, A.S. & Collins, J.J. Next-generation synthetic gene networks. *Nat. Biotechnol.* **27**, 1139–1150 (2009).
20. Davis, J.H., Rubin, A.J. & Sauer, R.T. Design, construction and characterization of a set of insulated bacterial promoters. *Nucleic Acids Res.* **39**, 1131–1141 (2011).
21. Mijakovic, I., Petranovic, D. & Jensen, P.R. Tunable promoters in systems biology. *Curr. Opin. Biotechnol.* **16**, 329–335 (2005).
22. Groth, A.C. & Calos, M.P. Phage integrases: biology and applications. *J. Mol. Biol.* **335**, 667–678 (2004).
23. Gordley, R.M., Gersbach, C.A. & Barbas, C.F. III. Synthesis of programmable integrases. *Proc. Natl. Acad. Sci. USA* **106**, 5053–5058 (2009).
24. Lux, M.W., Bramlett, B.W., Ball, D.A. & Peccoud, J. Genetic design automation: engineering fantasy or scientific renewal? *Trends Biotechnol.* **30**, 120–126 (2012).
25. Lu, T.K. & Collins, J.J. Engineered bacteriophage targeting gene networks as adjuvants for antibiotic therapy. *Proc. Natl. Acad. Sci. USA* **106**, 4629–4634 (2009).
26. Ortiz, M.E. & Endy, D. Engineered cell-cell communication via DNA messaging. *J. Biol. Eng.* **6**, 16 (2012).
27. You, L., Cox, R.S., Weiss, R. & Arnold, F.H. Programmed population control by cell-cell communication and regulated killing. *Nature* **428**, 868–871 (2004).
28. Bacchus, W. *et al.* Synthetic two-way communication between mammalian cells. *Nat. Biotechnol.* **30**, 991–996 (2012).
29. McMillen, D., Kopell, N., Hasty, J. & Collins, J.J. Synchronizing genetic relaxation oscillators by intercell signaling. *Proc. Natl. Acad. Sci. USA* **99**, 679–684 (2002).

## ONLINE METHODS

**Materials.** All experiments except for those involving the digital-to-analog converters were performed in Luria-Bertani (LB)-Miller medium (Fisher, #BP1426-2) using appropriate antibiotics at the following concentrations: carbenicillin (50 µg/ml), kanamycin (30 µg/ml) and chloramphenicol (25 µg/ml). All experiments involving the digital-to-analog converters were performed in LB-Miller medium (Fisher, #BP1426-2) using appropriate antibiotics at the following concentrations: carbenicillin (50 µg/ml), kanamycin (30 µg/ml) and chloramphenicol (35 µg/ml).

**Recombinase-based computation plasmid construction.** All plasmids were constructed using basic molecular cloning techniques<sup>30</sup> and Gibson assembly<sup>16</sup>. New England BioLabs (NEB) restriction endonucleases, T4 DNA Ligase and Phusion PCR kits were used. PCRs were carried out with a Bio-Rad S1000 Thermal Cycler with Dual 48/48 Fast Reaction Modules (Bio-Rad). Custom sequences, including recombinase recognition sites, were constructed from Integrated DNA Technologies (Coralville, IA).

All plasmids were transformed into *E. coli* strain DH5αPRO (F<sup>-</sup> φ80lacZΔM15 Δ(lacZYA-argF)U169 deoR recA1 endA1 hsdR17(r<sub>K</sub><sup>-</sup>, m<sub>K</sub><sup>+</sup>) phoA supE44 thi-1 gyrA96 relA1 λ<sup>-</sup>, P<sub>N25</sub>/tet<sup>R</sup>, P<sub>lacIq</sub>/lacI, Sp<sup>r</sup>) with standard protocols and isolated with Qiagen QIAprep Spin Miniprep Kits. Plasmid modifications were confirmed by restriction digests and sequencing by Genewiz (Cambridge, MA).

The promoter P<sub>Ltet0-1</sub> and the RBS in pZA31G were removed using excision by XhoI and KpnI and replaced with the same RBS and an EagI restriction site. All components for the recombinase-based computation devices that consisted of promoters and/or terminators located between recognition sites and a downstream *gfp* gene that was not sandwiched between recognition sites were then Gibson assembled between the AatII and XhoI restriction sites in pZA31G Cm<sup>R</sup>. All the other designs (i.e., those that involved *gfp* sandwiched between recognition sites) were Gibson assembled between AatII and AvrII restriction sites.

The *bx1* gene was a gift from the G.F. Hatfull lab and was cloned into a variant of the riboregulator vector rrjc12y(rii)g from Callura *et al.*<sup>13</sup> between the restriction sites KpnI and HindIII. This high-copy number plasmid contains kanamycin resistance and the P<sub>Lux</sub> promoter driving transcription of *trans*-activating RNA (taRNA) version taR12y and *bx1*. The *bx1* gene has the crR12y *cis*-repressive sequence upstream of the RBS.

The *phiC31* gene was obtained from Addgene plasmid 18941 (Cambridge, MA). The *phiC31* gene was cloned into a variant of the riboregulator vector rrjt12(11)g from Callura *et al.*<sup>13</sup> between the restriction sites KpnI and PstI. This medium-copy number plasmid contains carbenicillin resistance and the P<sub>Ltet0-1</sub> promoter driving transcription of both taRNA version taR12 and *phiC31*. The *phiC31* gene has the crR12 *cis*-repressive sequence upstream of the RBS.

**Gibson assembly.** Gibson assembly was used to join promoters (proA, proB and proD)<sup>20</sup>, terminators (T1)<sup>7</sup> and output gene (*gfp*)<sup>7</sup> modules (**Supplementary Table 1**) together to implement integrated logic and memory plasmids in single-step reactions.

DNA fragments that overlapped in sequence by ~40 bases were constructed by PCR through the design of PCR primers that contain 'overhangs', which provide sequence overlap with adjacent fragments. The protocol described by Gibson *et al.*<sup>16</sup> was followed. Briefly, Gibson assembly master mix was prepared by adding 320 µl of 5 × ISO buffer, 0.64 µl of 10 U/µl T5 exonuclease, 20 µl of 2 U/µl Phusion polymerase, 160 µl of 40 U/µl Taq ligase and water to bring it to

1.2 ml. Aliquots of 15 µl were prepared and then used for a single Gibson reaction. Next, 100 ng of the linearized vector backbone and equimolar amounts of the other assembly pieces were added to the 15 µl master mix in a 20 µl total volume assembly reaction mixture. The assembly reaction was incubated at 50 °C for 60 min, and then 5 µl of the assembly reaction was transformed into 100 µl of competent *E. coli*.

**Recombinase-based computation flow cytometer measurements.** Before performing flow cytometer measurements, cells were grown overnight in inducer-free medium and then diluted 1:1,000 in medium with the inducer anhydrotetracycline (Sigma) at a final concentration of 200 ng/ml and/or AHL at a final concentration of 1 µM, as indicated. The cells were grown for 4 h in inducer(s), washed, diluted 1:1,000 and grown overnight at 37 °C and 300 r.p.m. in inducer(s). Next the cells were centrifuged and washed in medium without inducer. Cells were then diluted 1:100 into a new 96-well plate containing fresh 1 × PBS and immediately assayed using a BD-FACS LSRFortessa-HTS cell analyzer (BD Biosciences, CA). FlowJo (Treestar, OR) was used for data analysis and visualization. Fluorescence was measured with a 488-nm argon laser excitation and a 515-nm to 545-nm emission filter. To ensure consistency between samples, 50,000 cells were collected for each sample and consistently gated by forward scatter (FSC) and side scatter (SSC). A consistent fluorescence threshold was applied to determine the percentage of cells deemed GFP<sup>+</sup> (ON state) or GFP<sup>-</sup> (OFF state) in **Figures 1–3** and **Supplementary Figure 2** (see example in **Supplementary Fig. 1**). The percentages of cells that expressed GFP are the averages over three independent experiments (**Figs. 1–3** and **Supplementary Fig. 2**). The mean fluorescence levels for the digital-to-analog converters in **Figure 4** (and the supporting experiments in **Supplementary Figs. 3** and **4**) are based on the geometric means from three independent experiments. Error bars for all experiments represent the s.e.m.

**Stable memory maintenance over multiple generations.** To study the temporal stability of our recombinase-based memory devices, cells containing an AND gate were induced from OFF to ON as described above. These cells were then repeatedly grown and diluted 1:2,000 every day in medium without inducer for 9 d to achieve ~11 generations per day. The ability of the cells to maintain their state was monitored by measuring the expression of GFP using flow cytometry as described above. We determined that our recombinase-based memory devices could hold their state for at least ~90 cell doublings. These data demonstrate the long-term operational stability of our recombinase-based memory devices.

**Stable memory maintenance after cell death.** Cells containing a NOR gate were exposed to no inputs, AHL alone, aTc alone, or both AHL and aTc overnight, centrifuged, washed and then killed by exposure to 90 °C for 30 min. PCR was performed on DNA isolated from the killed cells using EB Phusion PCR kits according to the manufacturer's instructions. PCRs were carried out with a Bio-Rad S1000 Thermal Cycler with Dual 48/48 Fast Reaction Modules (Bio-Rad). The PCR products were analyzed by electrophoresis on a 1% agarose gel.

**Primers.** The specific primers used (**Fig. 3**) were P1, GGC GCG TAC TCC TAA GAA AC; P2, TCT CCG TCG TCA GGA TCA TC; P3, ATT AAA GAG GAG AAA GGT ACC ATG C; and P4, AAA GTT AAA CAA AAT TAT TTG TAG AGG G.

30. Sambrook, J., Fritsch, E.F. & Maniatis, T. Molecular cloning: a laboratory manual. Cold Spring Laboratory Press 2 (1989).